

## RESEARCH ARTICLE

# Tensile properties and dynamic mechanical analysis of kenaf/epoxy composites

A. H. Abdullah<sup>1</sup>, I. Tharazi<sup>1</sup>, F. M. Salleh<sup>1\*</sup>, N. H. A. Halim<sup>1</sup>, Z. H. Solihin, A. P. Marzuki<sup>1</sup> and K. Abdan<sup>2</sup>

<sup>1</sup> School of Mechanical Engineering, College of Engineering, Universiti Teknologi MARA, 40450, Shah Alam, Selangor, Malaysia  
 Phone: +60355435052; Fax.: +60355435160

<sup>2</sup> Department of Biological and Agricultural, Faculty of Engineering, Universiti Putra Malaysia, 43400, Serdang, Malaysia

**ABSTRACT** - Kenaf fibre-reinforced polymer composites could offer low-cost, biodegradable, recyclable, and renewable materials. The hydrophilic kenaf fibres exhibit poor compatibility with the hydrophobic epoxy matrix as compared to their synthetic counterparts and ultimately, this may severely constrain their potential as a green composite material. This work aims to evaluate the tensile properties and dynamic mechanical analysis (DMA) of kenaf fibre composites reinforced with two epoxy systems as matrices, B and M resins. Neat epoxy samples and kenaf-reinforced composites with varying fibre loading, 15% and 45% were fabricated in the study. It was found that the tensile properties of kenaf composites are dependent on the epoxy resin systems and higher with reinforcement content. The tensile strength of M-15% and M-45% are 16.3% and 12.0% stronger than their counterparts. Determination of interfacial shear strength using a modified micromechanical model was employed showing that M-45 has a higher value than B-45%, 107.09 kPa and 90.28 kPa respectively. By DMA, in general, an increase in the storage modulus and peak height in the loss modulus was always higher with kenaf composites that were manufactured with the M resin system. The adhesion factor, A calculated from tan delta curves and cole-cole plot has shown the state of fibre/matrix adhesion level in each epoxy resin system. The SEM analysis indicates the presence of void spaces around fibres and matrix may attributed to the lower compatibility of the B resins system used in kenaf composites fabrication.

## ARTICLE HISTORY

Received : 26<sup>th</sup> June 2023

Revised : 19<sup>th</sup> Jan. 2024

Accepted : 27<sup>th</sup> Feb. 2024

Published : 30<sup>th</sup> Mar. 2024

## KEYWORDS

*Polymer composite*

*Kenaf fibre*

*Epoxy matrix*

*Tensile properties*

*DMA*

## 1. INTRODUCTION

Interest in the application of natural fibres as reinforcement in composites has increased in recent years. Natural fibres can offer benefits such as low weight, recyclability, and low cost compared to glass fibre. Current uses of natural fibre composites are limited to non-demanding applications such as the interior part of automotive but many researchers have shown that natural fibre composites can accommodate themselves in load-bearing applications such as small wind turbine blades [1] and car bumper beams [2]. The introduction of this kind of natural fibre-based composite in industries could provide manufacturers with a new alternative to generate economical green products with equivalent mechanical strength. Indirectly, the usage of natural fibre-based fibre could help reduce negative environmental impacts, such as air pollution, compared to synthetic fibre [3]. In this study, kenaf is used as the natural fibre and it is a native plant in tropical and subtropical Africa and Asia. There is growing interest in this plant in Malaysia because kenafs are rapidly growing and harvested twice a year in the local climate, making them suitable candidates as reinforcement in biocomposites [4].

Natural fibre composites are often reinforced with a thermoplastic or thermoset polymer matrix. Thermoset resins such as epoxy are widely chosen as matrix polymers in natural fibre composites because they are in the form of liquid, allowing the use of fabrics and mats as the fibre reinforcement [5] and exhibit excellent properties, such as strong chemical, thermal, electrical, and mechanical strength that makes this polymeric material gained in popularity over other materials [6]. Epoxy resin is a generic term to describe a three-membered cyclic ether group commonly denoted as an epoxy group [7]. The mechanical properties of epoxy resin are influenced by several factors such as pre-polymer structure, the curing agent, the stoichiometry between the resin and the hardener, curing time, and temperature [8]. In the case of natural fibre-reinforced epoxy composites, the most widely reported epoxy resin used is based on the diglycidyl ether of bisphenol A (DGEBA) and cured with amine-based hardener [9, 10].

The strength of fibre/matrix adhesions is one of the key factors in composites where it influences the final mechanical properties of composites. Unfortunately, hydrophilic and polar nature lignocellulose such as kenaf may have incompatibility issues with hydrophobic and non-polar polymer matrices, making weak formation of interface between fibre and matrix [11]. Thermoset resins such as epoxy and phenol could create stronger composites with natural fibres because of their ability to create covalent bonds with plant cell walls via hydroxyl groups. However, the presence of non-cellulosic constituents such as hemicellulose and lignin in fibre compositions could lower their mechanical performance [12]. The effect of matrix used on the mechanical performance of natural fibre composites is discussed in the literature. Madsen et al. [13] studied the effect of thermoplastic matrices composites on the tensile properties of hemp yarn-

reinforced composites. They found Polyethylene terephthalate (PET) composites were the highest, followed by Polyethylene (PE) and Polypropylene (PP) composites. The study between thermoset matrices polyester, epoxy and vinyl ester was explored by Joffe and co-workers [14] on the flax reinforcement in composites. They reported that differences in thermoset matrices resulted in different mechanical properties. These authors agreed that it could be the difference in the fibre/matrix bonding but claimed that it may not give any substantial result to the composite properties. It is believed that each epoxy resin manufacturer has their formulations to meet the demands of various industries. However, these formulations may be limited to certain applications such as adhesives, flooring, coatings, and laminates. As a result, it is possible that the compatibility of these hydrophobic epoxy resins with hygroscopic natural fibres may not always be taken into account by these manufacturers. This presents a challenge to optimise the performance and durability of natural fibre composite materials compared to their glass fibre composite counterparts.

The purpose of this study is to examine the compatibility between the fibres and the matrix of two commercially available epoxy resins used in the fabrication of kenaf fibre composites. The study also explored the impact of fibre loadings (15% and 45%) on kenaf/epoxy composites to better understand the role of reinforcement in developing stronger composites. The performance of the neat epoxy resins and their kenaf/epoxy composites was evaluated using tensile and dynamic mechanical analysis.

## 2. MATERIALS AND METHODS

### 2.1 Raw Materials

The kenaf fibres (unidirectional form) were obtained from the Institut Perhutanan Tropika dan Produk Hutan (INTROP), Universiti Putra Malaysia. In this study, commercial Bisphenol A diglycidyl ether (DGEBA) type epoxy resins were used, namely, BBT 7892 and Mirapox 950 were supplied by Berjaya Bintang Timur Sdn Bhd and Miracon Sdn Bhd. The epoxy mixing was performed with an amine-based hardener. Epoxy resin from these manufacturers was chosen because their product was often reported in the literature and is suitable for resin impregnation due to lower viscosity. The specific properties of the epoxy resin data sheets are shown in Table 1.

Table 1. Specific datasheet properties of epoxy resins

Properties	BBT 7892		Mirapox 950	
	Resin	Hardener	Resin	Hardener
Ingredients	DGEBA	3-aminomethyl-3,5,5-trimethylcyclohexylamine	DGEBA	Polyoxypropylene Diamine & Diethylenetriamine
Viscosity, CPS	10,300 @ 30°C	120 @ 30°C	7000-12,000 @ 25°C	350 – 600 @ 25°C
Mixing ratio, pbw	100:20		100:50	
Mix viscosity, CPS	N/A		Approx. 1000	

### 2.2 Fabrication of Composites

The hand-layup technique was used to fabricate the composites in a steel mould as shown in Figure 1(a). The fabrication began by aligning the fibres inside the mould cavity (23 mm in length x 17 mm in thickness x 50 mm in width) with different amounts of fibre  $V_f$ ; 0% (Neat), 15% and 45%, respectively are labelled as Neat B (BBT 7892), B-15%, B-45%, Neat M (Mirapox 950), M-15% and M-45%. Epoxy resin and hardener were mixed in a plastic cup according to the manufacturer's specifications as specified in Table 1. The mixture was slowly stirred with a wooden stick for about 4 minutes to minimise any potential bubble development in the mixture. The mixture was then carefully poured over the fibres, and the process was stopped when all the fibres were completely soaked by the resins.

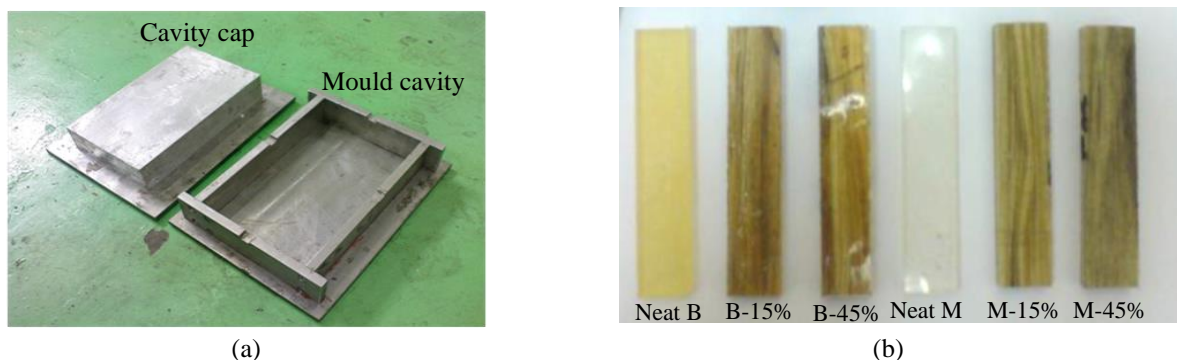


Figure 1. Photograph of: (a) steel mould for composites fabrication and (b) examples of cured samples

Next, the upper cavity cap was inserted on top of the mould and a compression force of 500 N was applied to close the mould using a cold press machine. The distance between the mould cavity and the cap cavity was limited by the use of metal spacers (4 mm in thickness), allowing excess liquid resin to be removed and ensuring uniform thickness of the samples. The samples were left for 24 hours to cure at room temperature. The cured plates were finally removed from the mould and cut using a band saw machine, and examples of the cured samples are shown in Figure 1(b).

### 2.3 Tensile Test

A tensile test was conducted following ASTM D-3039M using an Instron 3366 universal testing machine fitted with 10 kN load cells. The samples were cut into a rectangular geometry; 230 mm in length and 16 mm in width. The gauge length was marked 150 mm apart with aluminium tabs applied at both ends of the samples. Preliminary tests were performed to ensure that the grip was not slipped or damaged prematurely around the grip area. Samples were loaded at a constant crosshead rate of 2 mm/minute up to fracture in a temperature-controlled laboratory. A total of six specimens were tested for each system. Young's modulus (in the linear strain range between 0.05-0.10 %), tensile strength, and tensile strain were calculated using Instron Bluehill 3 software.

### 2.4 Dynamic Mechanical Analysis

Dynamic mechanical analysis was performed using a DMA Q800 model (TA Instruments) to measure storage modulus,  $E'$ , loss modulus,  $E''$  and damping factor ( $\tan \delta$ ). The width and length of the samples were 12 mm and 50 mm, respectively. The test was run in dual cantilever mode under a fixed oscillating frequency of 1 Hz. The temperature was ramped from 25 °C to 100 °C at a constant heating rate of 5 °C/minute. Six specimens from each configuration were repeated for the DMA test. The data of the storage modulus,  $E'$ , loss modulus,  $E''$  and  $\tan \delta$  were recorded against temperature. Data were analysed using Universal Analysis 2000 software (TA Instruments). The glass transition temperature,  $T_g$  of the samples was determined from the peak of the tan delta curves.

### 2.5 Surface Morphology

The fractured surface of the composites was examined using a Phillips XL 30 ESEM scanning electron microscope (SEM). Using a stub, the sample was mounted on a carbon adhesive tape and then coated 24 hours with platinum-gold using a sputter coater prior to imaging. The SEM operated at an acceleration voltage of 10.0 kV and a constant pressure of 0.8 Torr was maintained during the examination. The working distance between 8.0 mm and 12.00 mm was selected for optimised viewing experiences.

## 3. RESULTS AND DISCUSSION

### 3.1 Tensile Properties

Figure 2 shows the typical stress-strain of the composites. The mean tensile strength and Young's modulus are plotted as shown in Figure 3 and. It can be seen in Figure 2 that the curves started with a straight line, representing the pure elastic properties of the materials. The differences between Neat B resin and Neat M resin are obvious where the former failed abruptly at the maximum tensile loading. In contrast, the latter had a maximum curve peak at approximately 25 MPa and, subsequently, the samples elongated further before completely failing (~3.5 % of tensile strain). This suggests that Neat M samples experienced a non-linear plastic deformation towards the final fracture, suggesting a non-recoverable after the unloading phase. The increasing fibre content in the composites; B-15 %, M-45 %, M-15 % and M-45 % resulted in higher curve gradients and tensile strength, suggesting an improvement in load transfer efficiency. The improvement in tensile properties in the investigation as a result of the increase in the proportion of reinforcement is consistent with other reported research [15, 16].

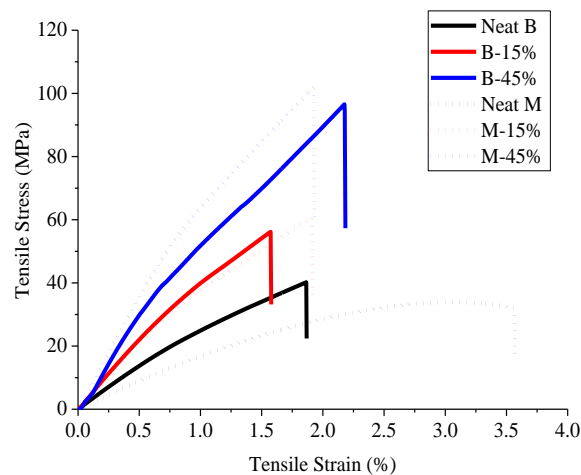


Figure 2. Typical tensile stress-strain curves of Neat epoxy and its composites

As shown in Figure 3, it is clear that the Neat M composite has lower tensile strength than the Neat B composite, 36.59 MPa and 32.19 MPa respectively. However, the addition of 15% and 45% kenaf fibre loading indicates that M-15 % and 45 % have stronger tensile strength with respect to B-15 % and B-45 % composites. The improvement in tensile strength is about 16.3 % and 12.0 %. The variation of Young’s modulus of composites (Figure 3) closely matches of tensile strength shown in Figure 4. The Neat M composites have the lowest Young’s modulus of 1.84 GPa compared to the Neat B composite, which is higher at 2.98 GPa. While the composites with 15% fibre volume content (B-15 % and M-15 %) show comparable stiffness at 4.62 GPa and 4.36 GPa respectively, it is interesting to observe that M-45% resulted highest modulus than the B-45 %, 8.12 GPa and 7.49 GPa for which the improvement is up to 12.0 %. Shah [15] explained that fibres in unidirectional or continuous fibre composites carry most of the load where the fibre/matrix interface would have little effect on the longitudinal tensile properties. However, in this study, there is a substantial improvement effect of using M resins in the manufacture of kenaf fibre composites fabrication. This effect has not arisen from the strength and modulus of the matrix alone. Part of the discrepancy can be explained by the fact that there is a potential difference in fibre/matrix compatibility between composites fabricated with epoxy B and M resin systems.

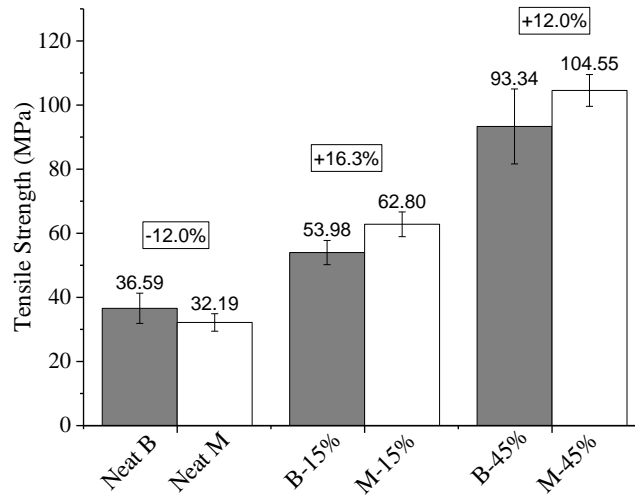


Figure 3. Tensile strength of composites

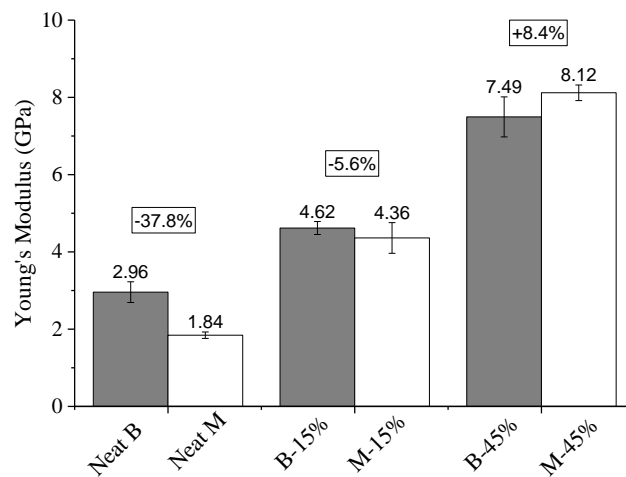


Figure 4. Young’s modulus of composites

Assessing fibre/matrix interfacial bonding in unidirectional and continuous composites is not straightforward because the traditional Voigt model or known rule of mixture (ROM) assumes the interfacial strength of a composite is nearly perfect. A back-calculated method using a modified ROM micromechanical model for short fibre composites is used in this study to determine the state of interfacial shear strength,  $\tau$  between fibre and matrix. The tensile strength of composites is estimated by the following equations [17]:

$$\sigma_c = \tau V_f \frac{1}{d} + \sigma_m (1 - V_f) \tag{1}$$

where  $\sigma_c$  and  $\sigma_m$  are the tensile strength of the composite and matrix.  $V_f$  is fibre volume fraction while  $\frac{1}{d}$  is the fibre aspect ratio. The micromechanical model assumes fibre length is lower than its critical length and that the composite strength depends on the fibre volume fraction, fibre/matrix interfacial strength and tensile strength of the matrix. Figure 5 shows

the back-calculated interfacial shear strength of composites. It is observed that M-15 % has a higher interfacial shear strength than B-15 % with an improvement of about 42 %. A similar enhancement is also observed for M-45 % where the back-calculated interfacial shear strength is 107.09 kPa, while B-45 % has a lower value at 90.28 kPa. This implies that the fibre/matrix interfaces differ for each epoxy matrix in this study. The result is in agreement with the tensile strength values in Figure 3.

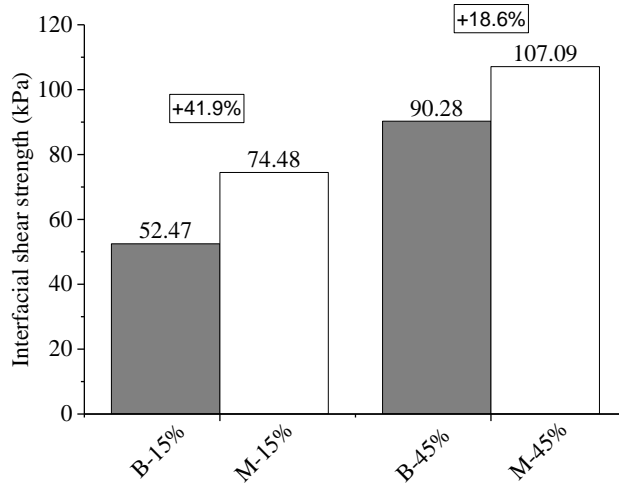


Figure 5. Interfacial shear strength of composites

### 3.2 Dynamic Mechanical Analysis

#### 3.2.1 Storage modulus

The variation of storage modulus at different temperatures of the composites is shown in Figure 1. In general, all curves were reduced with increasing temperature. A sudden decrease in storage modulus curves indicates a transition between the glassy region and the rubbery plateau region. The storage modulus of the samples is found to increase with increasing fibre content. This trend is expected due to the increase in the stiffness of the matrix with the reinforcement effect [18]. The storage modulus is lower for Neat M than for Neat B resin up to 70 °C. The result is consistent with Young’s modulus value, indicating a stronger Neat B polymer matrix. In the case of kenaf fibre composites, a similar observation is found for 15 % fibre content where the modulus of storage of B-15 % is higher than M-15 %. There is a sudden drop in storage modulus at early temperature (55 °C) of M-15% versus B-15 %, indicating the weak thermal resistance of the composites. This could be due to the lower glass temperatures,  $T_g$  of the M resins. However, at high fibre loading, it appears that the storage modulus of M-45 is greater than B-45 % at all measured temperatures, including in the rubbery region. It is well known in the literature that any alteration in adhesion properties between the fibres and the surrounding epoxy polymer could affect DMA responses [19]. A difference in the storage modulus of neat epoxy samples (Neat B vs. Neat M) compared to samples with 45 % fibre loading (B-45 % vs. M-45 %) could suggest that the adhesion between the fibres and matrix is more significant than the strength of the epoxy matrix alone in creating stronger natural fibre composites.

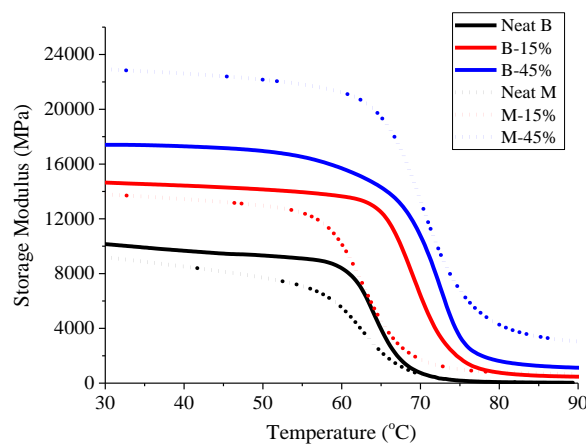


Figure 1. Typical curve storage modulus of composites

#### 3.2.2 Loss modulus

Figure 7 shows a variation of the loss modulus as a function of the temperature of the tested samples. It is clear that from Figure 7, the Neat N, N-15 % and B-45 % have consistent loss modulus height which is around 1600 MPa, while

there is a substantial modulus increment with fibre loading at the loss modulus height for Neat M, M-15 % and M-45 %. The increase in the loss modulus can be attributed to enhanced internal friction that increases the dissipation energy [20]. In this case, internal friction was considered greater for M-45 % compared to B-45 %, leading to stronger composites. The peak of the loss modulus curve usually determines the glass transition,  $T_g$  of the composites shown in Figure 8.  $T_g$  indicates the relaxation in a polymer where a material changes from a glass state to a rubber state. As illustrated in Figure 8, Neat B has higher  $T_g$  than Neat M, translating to the higher cross-linked density of unreinforced epoxy samples. This result agrees with the higher storage modulus value of Neat B compared to Neat M (Figure 7). There is an increase in  $T_g$  with increasing fibre volume fraction for the samples, which can be seen in Figure 8. An increase in glass transition in fibrous composites can be associated with decreased mobility of polymer chains by fibre addition [21]. Pothan et al. [22] found a positive relationship between the shift of  $T_g$  and fibre/matrix interaction in composites. A greater shift of  $T_g$  may indicate a better fibre/matrix interaction in composites. In present investigations, the shift of  $T_g$  at 8 °C between Neat B and B-15 % is observed in Figure 8. In a comparison of composites fabricated using M resins, a significant  $T_g$  shift between M-15 % and M-45 % is noticeable which is the highest, 10 °C. This could explain the higher storage modulus value of B-15 % versus M-15 % and M-45 % versus B-45 %, as illustrated in Figure 8.

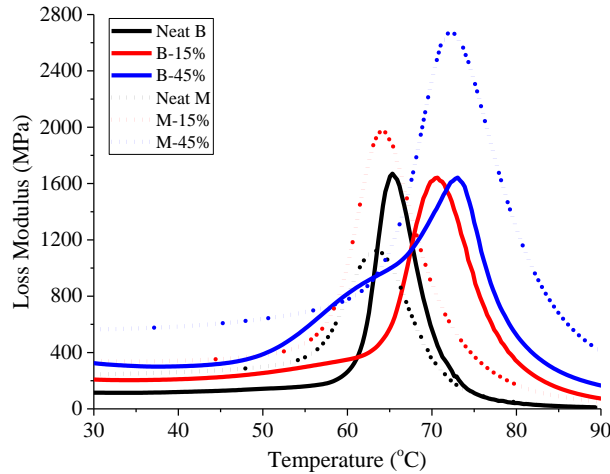


Figure 7. The loss modulus of composites

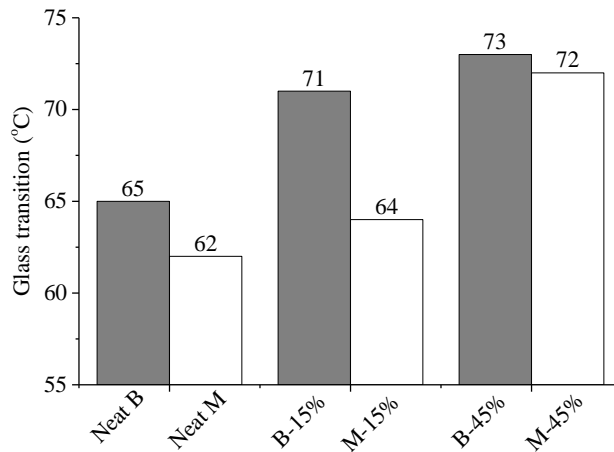


Figure 8. Glass transition of composites

### 3.3.3 Tan delta

The damping properties are given as tan delta and shown in Figure 9. The lowering tan delta height upon fibre loading for both types of composites suggests there is a restriction of movement of polymer molecules as a result of embedded fibre at the fibre/matrix interface. In the 15 % fibre content, not much variation of tan delta height was observed but significant changes are seen at the 45 % fibre volume content. The lower Tan delta height of M-45 % than B-45 % indicates stronger composites, corresponding to good interfacial adhesion which possibly resulted from enhanced chemical bonding interaction of fibre contact areas with the composite fabricated with the M resin system.

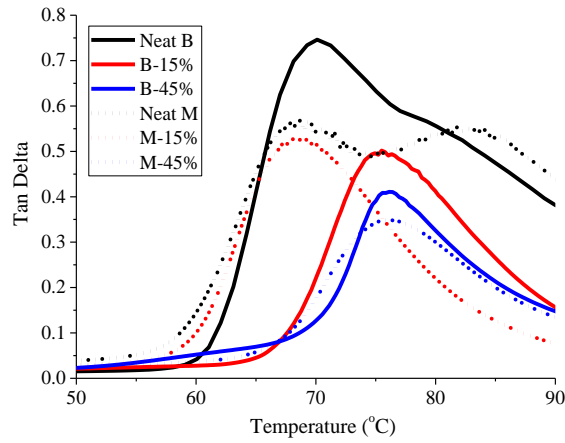


Figure 9. Tan delta of composites

### 3.3.4 Adhesion Factor ‘A’

The earliest attempt to measure the adhesion strength quantitatively using composite damping properties ( $\tan \delta$ ) was proposed by Kubat et al. [23] on high-density polyethylene filled with 20 vol% glass fibre. This model assumed that the summation of each damping property component corresponds to each constituent's volume fraction. This model accounts for the effect interface in composites which is not being considered by the conservative rule of mixture [24]. The summation of mechanical damping properties is given as follows:

$$\tan \delta_c = V_f \tan \delta_f + V_i \tan \delta_i + V_m \tan \delta_m \tag{2}$$

where, the subscript of  $f$ ,  $i$ , and  $m$  donates fibre, interface, and matrix respectively. By assuming the volume of  $\tan \delta_f$  is rather small, it can be neglected and the Eq. (2) is now can be written as follows:

$$\frac{\tan \delta_c}{\tan \delta_m} \approx (1 - V_f)(1 + A) \tag{3}$$

$$A = \frac{V_i}{1 - V_f} \frac{\tan \delta_i}{\tan \delta_m} \tag{4}$$

By arranging the Eq. (4), the Adhesion Factor ‘A’ can be calculated in terms of the damping properties of composites and matrix at a temperature is given as follows:

$$A = \frac{1}{1 - V_f} \frac{\tan \delta_c}{\tan \delta_m} - 1 \tag{5}$$

The adhesions factor ‘A’ shows an increased value if there is a decrease in molecular mobility near the interface, indicating a lower degree of fibre/matrix adhesion [25].

The interaction between epoxy matrices and their kenaf/epoxy composites was tracked using adhesion factor ‘A’ as shown in Figure 10. The B-15 % has lower adhesion factors ‘A’ than M-15% e below the glass transition temperature. In contrast, it seems that by increasing fibre content up to 45 %  $V_f$ , the M-45% has a lower ‘A’ than the B-45 %. To describe this, it is important to acknowledge that the fibre/matrix adhesion strength may not change in the event of varying fibre content but rather it may increase the interfacial area per unit volume of material [18].

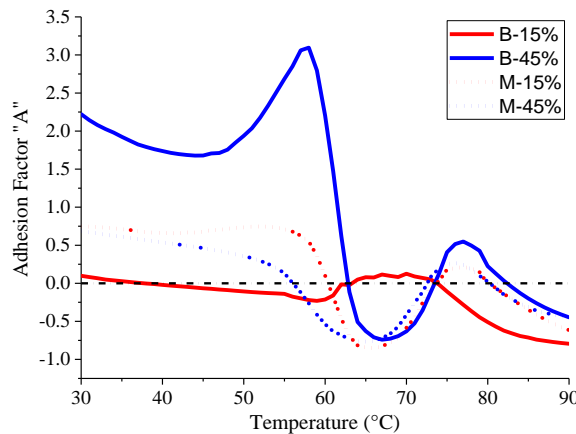


Figure 10. Adhesion factor ‘A’ versus temperature of composites

So, according to this concept, the adhesion factor ‘A’ should remain the same and this can be evidently seen in Figure 10 where the adhesion factor ‘A’ values for M-15 % and M-45 % are almost similar. On the contrary, the increased fibre content caused adhesion factor ‘A’ of B-45 % to be significantly higher as compared to the B-15 %. Given that there are changes in interfacial adhesions with a higher fibre content using a B epoxy resin system, those results can be explained in terms of poor resin impregnation for B-45 %. The argument is also supported by the observation that there is a sharp rise and sudden downturn of adhesion factor ‘A’ of the B-45 % sample towards the glass transition temperature as compared to other B-15 % samples, suggesting there is an increased polymeric chain mobility of the fibre surface compared to the matrix [25].

It is believed that a small part of the effect is due to the increased void content. The SEM imaging of fractured surfaces between B-45 % and M-45% are shown in Figure 11(a) and Figure 11(b). Two types of porosity can be seen in SEM images. The first is void in the rich-resin region which seems in the perfect circular geometry and has a large diameter. This happened due to entrapped air during the resin impregnation. The second type of porosity is void spaces around fibres and matrix which resulted from poor fibre/matrix interface. The qualitative observation shows that this kind of void was frequently found in the B-45 % as opposed to M-45 %. Therefore, it is believed that the combination of closely packed kenaf fibre and low compatibility of the B resin system may provide less fibre wetting during the resin filling stage.

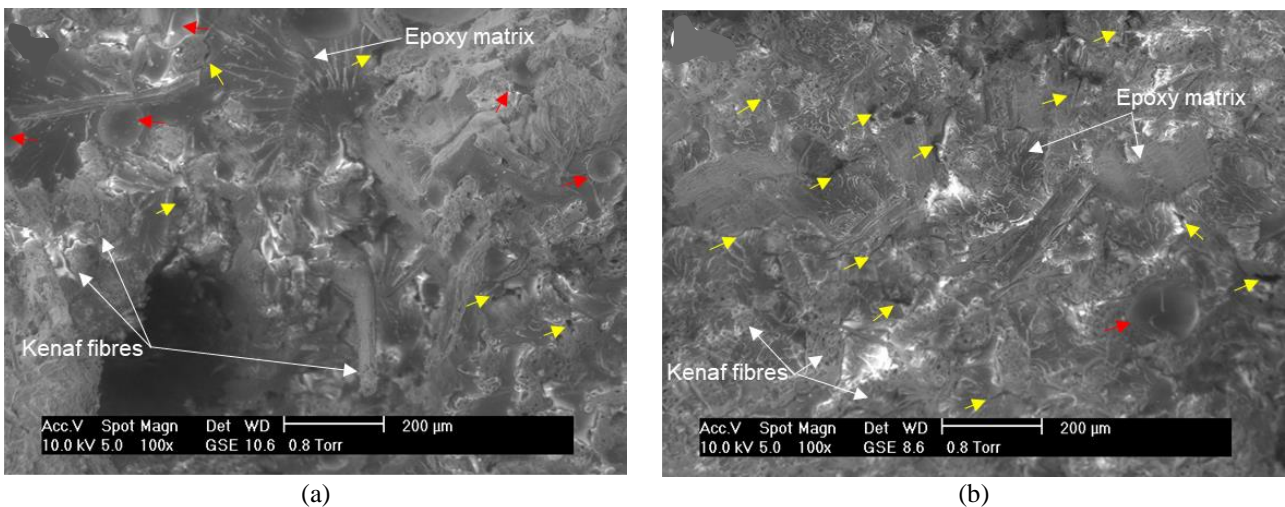


Figure 11. Qualitative observation of porosity in composites; (a) M-45 % and (b) B-45 %. Red arrows locate voids in matrix-rich regions while yellow arrows indicate void spaces around fibre and matrix

### 3.3.5 Cole-cole plot

The Cole-cole diagrams were plotted in terms of loss modulus against storage modulus to understand the structural changes of the polymer after the addition of fibres [26] and the intensity of the fibre/matrix interaction [22]. A perfect semi-circle diagram indicates a homogeneity of the polymeric system [21]. The Cole-cole plot between neat epoxy and their kenaf fibre composites is shown in Figure 12. Figure 12 shows that Neat B and Neat M exhibit imperfect semi-circle curves indicating the heterogeneity nature of the epoxy polymer. With fibre reinforcement in epoxy matrices, the degree of heterogeneity decreases with increasing fibre content from 15 % to 45 %. The curve of M-45 % shows the lowest degree of heterogeneity when compared to the B-45 %, implicating greater fibre/matrix interaction.

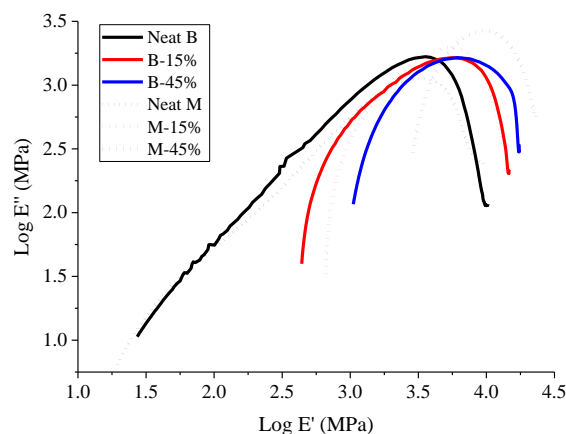


Figure 12. Cole-cole plot of composites

#### 4. CONCLUSIONS

In this study, the influence of two epoxy resin systems (B and M resins) and their kenaf fibre composites on the tensile properties and dynamic mechanical analysis was investigated. The study also considered the effect of fibre volume fraction, 15 % and 45 %. The mechanical properties of neat M are lower than Neat B in the unreinforced system. Regarding the fibre volume fraction, the tensile properties of kenaf fibre composites were highly dependent on the epoxy resins system. A back-calculated using a modified rule-of-mixtures model demonstrates the increased tensile properties of the kenaf fibre composites reinforced with a B resin system are correlated to enhanced interfacial shear strength. In terms of the DMA test, there was a great influence on fibre loading and the epoxy resin system used in the kenaf composite fabrications, showing the storage modulus is the highest for M-45 % over the temperatures. The loss modulus curves were found to distribute a wider range and reach higher values for the case of kenaf composites fabricated with the M resins system. This means there is an increased internal friction and dissipation energy in these composites. An adhesion factor, A determined from tan delta curves had shown a lower and consistent value in the M-15 % and M-45 %, indicating interfacial area per unit volume of material remains consistent despite an increase in fibre loading. The compatibility of epoxy resins was evidenced by the SEM images. More void spaces around fibres and matrices were found in the B-45 % as opposed to M-45 %, indicating poor fibre-wetting.

#### 5. ACKNOWLEDGMENTS

The authors are grateful to the Research Management Centre of Universiti Teknologi MARA, Shah Alam for funding this project through 600-RMC/MYRA 5/3/LESTARI (124/2020).

#### 6. REFERENCES

- [1] D. U. Shah, P. J. Schubel, M. J. Clifford, "Can flax replace E-glass in structural composites? A small wind turbine blade case study," *Composites Part B: Engineering*, vol. 52, pp. 172–181, 2013.
- [2] M. M. Davoodi, S. M. Sapuan, D. Ahmad, A. Ali, A. Khalina, M. Jonoobi, "Mechanical properties of hybrid kenaf/glass reinforced epoxy composite for passenger car bumper beam," *Materials and Design*, vol. 31, no. 10, pp. 4927–4932, 2010.
- [3] I. Yusuff, N. Sarifuddin, S. Norbahiyah, A. M. Ali, "Mechanical properties, water absorption, and failure analyses of kenaf fiber reinforced epoxy matrix composites," *IJUM Engineering Journal*, vol. 22, no. 2, pp. 316–326, 2021.
- [4] J. Summerscales, N. P. J. Dissanayake, A. S. Virk, W. Hall, "A review of bast fibres and their composites. Part 1 – Fibres as reinforcements," *Composites Part A: Applied Science and Manufacturing*, vol. 41, no. 10, pp. 1329–1335, 2010.
- [5] A. Crosky, N. Soatthiyanon, D. Ruys, S. Meatherall, S. Potter, "Thermoset matrix natural fibre-reinforced composites," *Natural Fibre Composites: Materials, Processes and Applications*, Woodhead Publishing, pp. 233–270, 2014.
- [6] O. A. Shabeeb, D. S. Mahjoob, H. M. Mahan, M. M. Hanon, "Mechanical and thermal conductive properties of natural and synthetic cellulose reinforced epoxy composites," *IJUM Engineering Journal*, vol. 23, no. 2, pp. 193–204, 2022.
- [7] S. H. Lee, H. O. Choi, J. S. Kim, C. K. Lee, Y. K. Kim, C. S. Ju, "Circulating flow reactor for recycling of carbon fiber from carbon fiber reinforced epoxy composite," *Korean Journal of Chemical Engineering*, vol. 28, no. 2, pp. 449–454, 2011.
- [8] Z. Achmad, A. E. Ismail, A. Hamdan, "The effect of a mixture of epoxy resin matrix composite materials and hardener by varying the stirring speed on the mechanical properties," *International Journal of Engineering Trends and Technology*, vol. 69, no. 11, pp. 83–88, 2021.
- [9] V. O. Startsev, M. P. Lebedev, K. A. Khrulev, M. V. Molokov, A. S. Frolov, T. A. Nizina, "Effect of outdoor exposure on the moisture diffusion and mechanical properties of epoxy polymers," *Polymer Testing*, vol. 65, pp. 281–296, 2018.
- [10] A. Le Duigou, A. Kervoelen, A. Le Grand, M. Nardin, C. Baley, "Interfacial properties of flax fibre-epoxy resin systems: Existence of a complex interphase," *Composites Science and Technology*, vol. 100, pp. 152–157, 2014.
- [11] K. I. Ejiogu, U. Ibeneme, G. O. Tenebe, M. D. Ayo, M. O. Ayejagbara, "Natural fibre reinforced polymer composite (NFRPC) from waste polypropylene filled with coconut flour," *International Journal of Engineering Technology and Sciences*, vol. 6, no. 2, pp. 50–64, 2019.
- [12] R. Sepe, F. Bollino, L. Boccarusso, F. Caputo, "Influence of chemical treatments on mechanical properties of hemp fiber reinforced composites," *Composites Part B: Engineering*, vol. 133, pp. 210–217, 2018.
- [13] B. Madsen, P. Hoffmeyer, H. Lillholt, "Hemp yarn reinforced composites – II. Tensile properties," *Composites Part A: Applied Science and Manufacturing*, vol. 38, no. 10, pp. 2204–2215, 2007.

- [14] R. Joffe, L. Wallstrom, L. A. Berglund, "Natural fiber composites based on flax-matrix effects," in *International Scientific Colloquium*, Riga, Latvia, May 17-18, 2001, pp. 54–59.
- [15] D. Upendra Shah, "Characterisation and optimisation of the mechanical performance of plant fibre composites for structural applications," *Ph.D. Thesis*, University of Nottingham, UK, 2013.
- [16] M. S. Haque, I. A. Ovi, F. S. Prome, A. Hossain, "Impact of water absorption on tensile strength: A comparative study of jute fiber composites with various fiber content," *Malaysian Journal on Composites Science and Manufacturing*, vol. 12, no. 1, pp. 114–124, 2023.
- [17] A. Orue, A. Jauregi, U. Unsuain, J. Labidi, A. Eceiza, A. Arbelaiz, "The effect of alkaline and silane treatments on mechanical properties and breakage of sisal fibers and poly(lactic acid)/sisal fiber composites," *Composites Part A: Applied Science and Manufacturing*, vol. 84, pp. 186–195, 2016.
- [18] H. S. P. Da Silva, H. L. Ornaghi Júnior, J. H. Santos Almeida Júnior, A. J. Zattera, S. Campos Amico, "Mechanical behavior and correlation between dynamic fragility and dynamic mechanical properties of curaua fiber composites," *Polymer Composites*, vol. 35, no. 6, pp. 1078–1086, 2014.
- [19] A. Saeedi, R. Eslami-Farsani, H. Ebrahimnezhad-Khaljiri, M. Najafi, "Dynamic mechanical analysis of epoxy/natural fiber composites," *Handbook of Epoxy/Fiber Composites*, pp. 1–28, 2022.
- [20] N. Hameed, P. A. Sreekumar, B. Francis, W. Yang, S. Thomas, "Morphology, dynamic mechanical and thermal studies on poly(styrene-co-acrylonitrile) modified epoxy resin/glass fibre composites," *Composites Part A: Applied Science and Manufacturing*, vol. 38, no. 12, pp. 2422–2432, 2007.
- [21] M. Idicula, S. K. Malhotra, K. Joseph, S. Thomas, "Dynamic mechanical analysis of randomly oriented intimately mixed short banana/sisal hybrid fibre reinforced polyester composites," *Composite Science and Technology*, vol. 65, no. 7–8, pp. 1077–1087, 2005.
- [22] L. A. Pothan, S. Thomas, G. Groeninckx, "The role of fibre/matrix interactions on the dynamic mechanical properties of chemically modified banana fibre/polyester composites," *Composites Part A: Applied Science and Manufacturing*, vol. 37, no. 9, pp. 1260–1269, 2006.
- [23] J. Kubát, M. Rigdahl, M. Welander, "Characterization of interfacial interactions in high density polyethylene filled with glass spheres using dynamic-mechanical analysis," *Journal of Applied Polymer Science*, vol. 39, no. 7, pp. 1527–1539, 1990.
- [24] C. A. Correa, C. A. Razzino, E. Hage, "Role of maleated coupling agents on the interface adhesion of polypropylene-wood composites," *Journal of Thermoplastic Composite Materials*, vol. 20, no. 3, pp. 323–339, 2007.
- [25] H. L. Ornaghi, A. S. Bolner, R. Fiorio, A. J. Zattera, S. C. Amico, "Mechanical and dynamic mechanical analysis of hybrid composites molded by resin transfer molding," *Journal of Applied Polymer Science*, vol. 118, no. 2, pp. 887–896, 2010.
- [26] L. He, F. Xia, Y. Wang, J. Yuan, D. Chen, J. Zheng, "Mechanical and dynamic mechanical properties of the amino silicone oil emulsion modified ramie fiber reinforced composites," *Polymers*, vol. 13, no. 23, p. 4083, 2021.